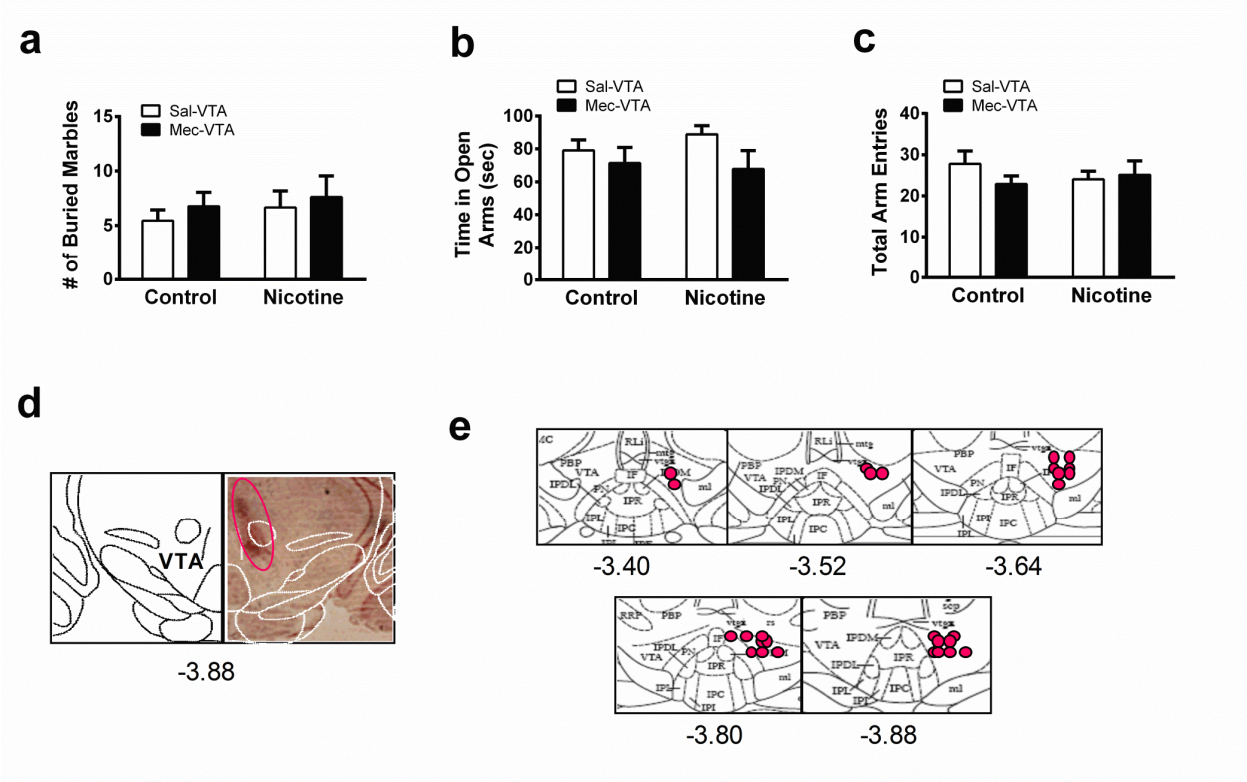

Supplementary Figure 1. Verification of drug infusions into the IPN. **a.** Representative neutral red-stained coronal section from a mouse with a guide cannula targeting the IPN. The guide cannula scar is circled in magenta (note that the infusion cannula projects 0.25 mm beyond the guide cannula). The stereotactic coordinates from bregma in mm are indicated below the photo. Brain atlas demarcations are overlaid onto the coronal section (white lines). **b.** Each magenta circle represents an individual guide cannula placement for a mouse that received micro-infusions into the IPN. Note that for clarity, not every cannula placement is shown. Guide cannula placements were verified as indicated in Methods and Results sections.

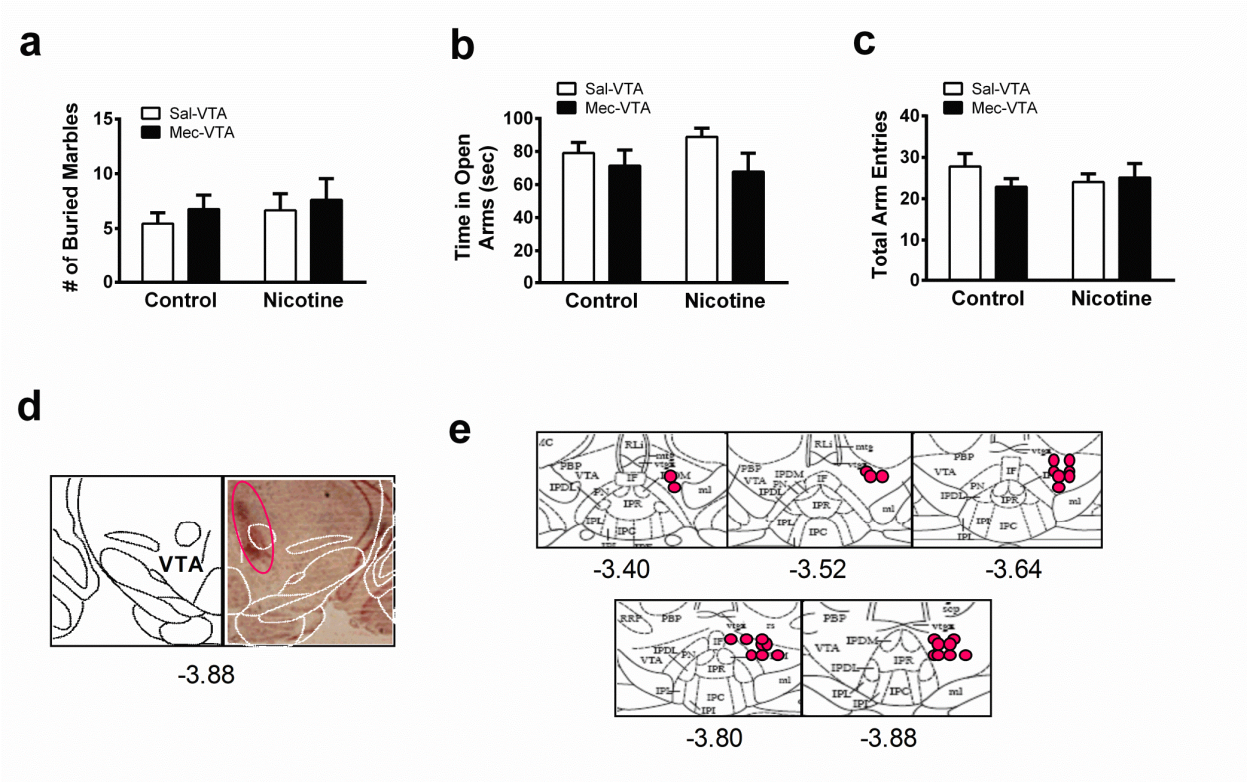

Supplementary Figure 2. Mecamylamine infusion into the VTA does not induce anxiety in nicotine-dependent mice. **a.** Average number of marbles buried in control and chronic nicotine treated mice after saline (1.5 μl, n = 9 mice/group) or mecamylamine (3 μg, n = 9 and 8, respectively) infusion into the VTA. **b**. Average time spent in the open arms of the EPM in control or chronic nicotine-treated mice after a VTA infusion of saline (n = 9 mice/group) or mecamylamine (n = 9 and 8, respectively). **c.** Average total arm entries in control or chronic nicotine treated animals after a VTA infusion of saline or mecamylamine as in panel b. **d.** Illustration depicting a mouse brain coronal section. Guide cannula scar is circled. **e.** Each magenta circle represents an individual guide cannula placement for a mouse that received micro-infusions into the VTA. Guide cannula placements were verified as in Fig. S2. Data are expressed as mean ± SEM.

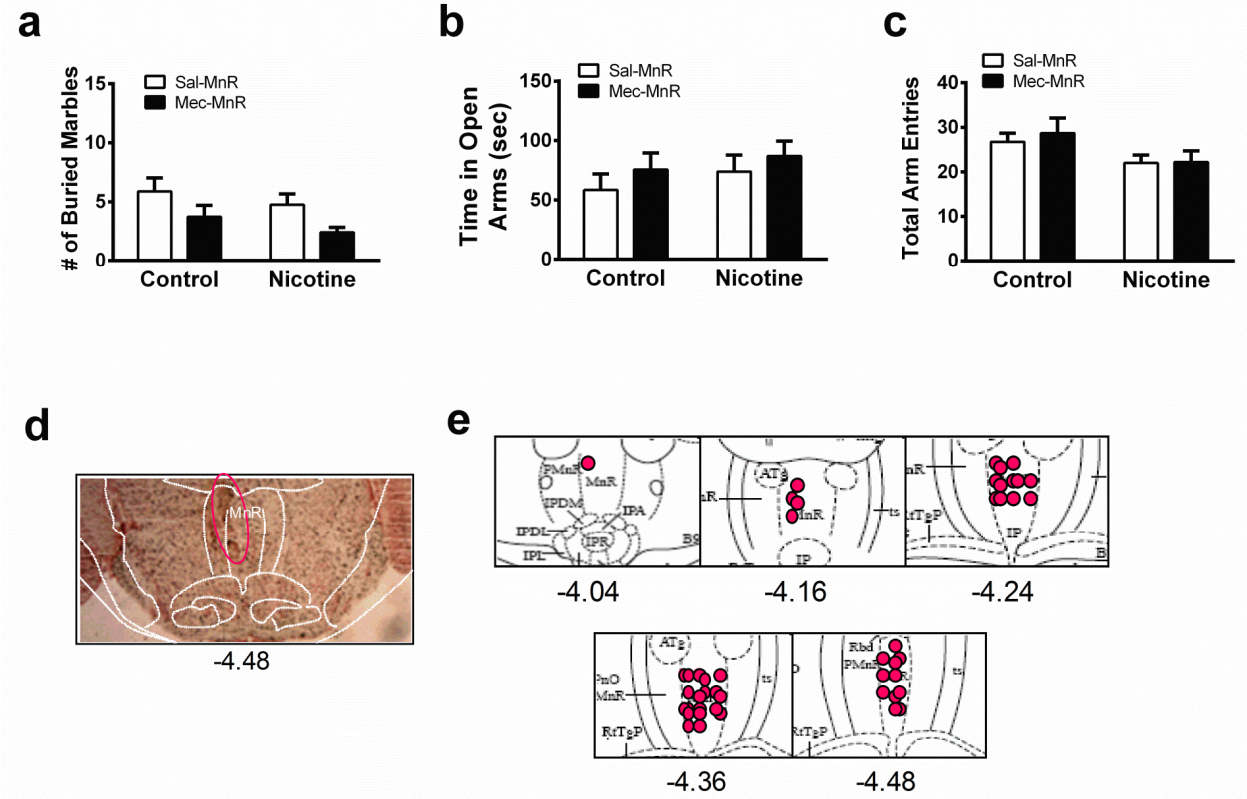

Supplementary Figure 3. Mecamylamine infusion into the MnR does not induce anxiety in nicotine-dependent mice. **a.** Average number of marbles buried in control and chronic nicotine treated mice after saline (1.5 μl, n = 8 mice/group) or mecamylamine (3 μg, n = 11 and 10, respectively) infusion into the MnR. Two-way ANOVA: significant effect of infusion ($F_{1,33}$ = 6.23, p = 0.018) but not chronic treatment nor an interaction. **b**. Average time spent in the open arms of the EPM in control or chronic nicotine-treated mice after a MnR infusion of saline (n = 8 mice/group) or mecamylamine (n = 11 and 10, respectively). **c.** Average total arm entries in control or chronic nicotine-treated animals. **d.** Illustration depicting a mouse brain coronal section. Guide cannula scar is circled. **e.** Each magenta circle represents an individual guide cannula placement for a mouse that received micro-infusions into the MnR. Guide cannula placements were verified as in Supplementary Fig. 2. Data are expressed as mean ± SEM.

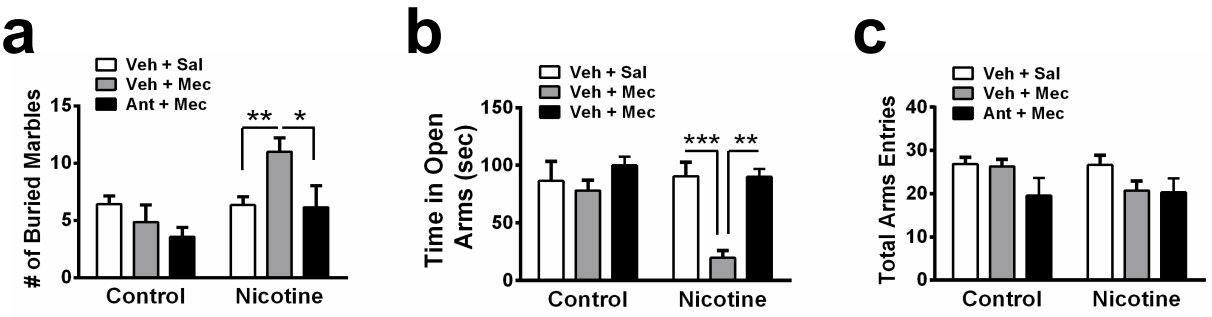

Supplementary Figure 4. Systemic antalarmin reduces anxiety during nicotine withdrawal. **a.** Average number of marbles buried in control and chronic nicotine-treated mice after an i.p. injection of vehicle (n = 24 mice/group) or antalarmin (10 mg/kg, n = 7 mice/group) prior to i.p. saline or mecamylamine (3 mg/kg). Two-way ANOVA: Chronic treatment $F_{1, 69}$ = 8.795, p = 0.0041, treatment x drug interaction $F_{2, 69}$ = 4.26, p = 0.018. **b.** Average time spent in the open arms of the EPM in control or chronic nicotine-treated mice after an i.p. injection of vehicle (n = 10 and 11, respectively) or antalarmin prior (n = 14 and 7, respectively) to i.p. saline or mecamylamine. Two-way ANOVA: Drug $F_{2, 50}$=8.82, p = 0.0005, Chronic treatment $F_{1, 50}$=4.83, p = 0.033, treatment x drug interaction $F_{2, 50}$ = 4.09, p = 0.023. **c.** Average total arm entries in control or chronic nicotine-treated animals after an i.p. injection of saline or antalarmin prior to i.p. saline or mecamylamine. Two-way ANOVA: Drug $F_{2, 50}$=3.76, p = 0.03. Data are expressed as mean ± SEM. *p<0.05, ** p < 0.01, *** p<0.01. ^p<0.05 compared to control mice under the same conditions.

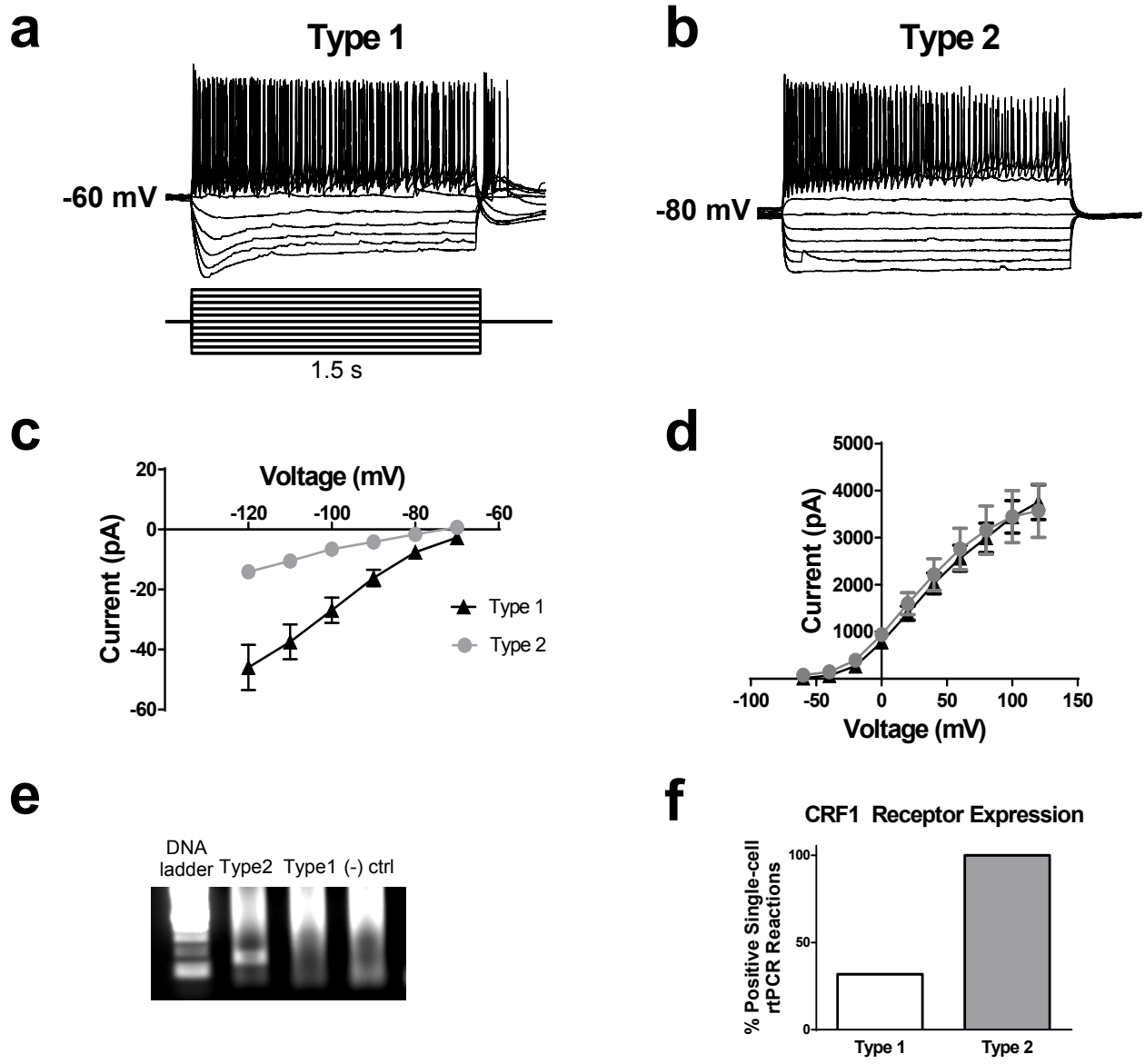

Supplementary Figure 5. Characterization of IPI neurons. Representative family of voltage traces from **a.** IPI Type 1 and **b.** IPI Type 2 neurons under current clamp. From resting membrane potential, current was injected in 10 pA steps for 1.5 s as indicated. **c.** Current-voltage relationship of Type 1 and Type 2 IPI neurons at hyperpolarized potentials between -70 and -120 mV (n = 10-13 neurons/Type). **d.** Current-voltage relationship of Type 1 and Type 2 IPI neurons from potentials between -60 and 120 mV

(n = 10-13 neurons/type). **e.** Representative gel illustrating CRF1 receptor expression from a single Type 1 and Type 2 neuron measured via RT-PCR after patch-clamp recording. **f.** Bar graphs indicate percent of patch-clamped Type 1 or Type 2 neurons that expressed CRF1 receptor mRNA as measured by single neuronal RT-PCR. Data are expressed as mean ± SEM.

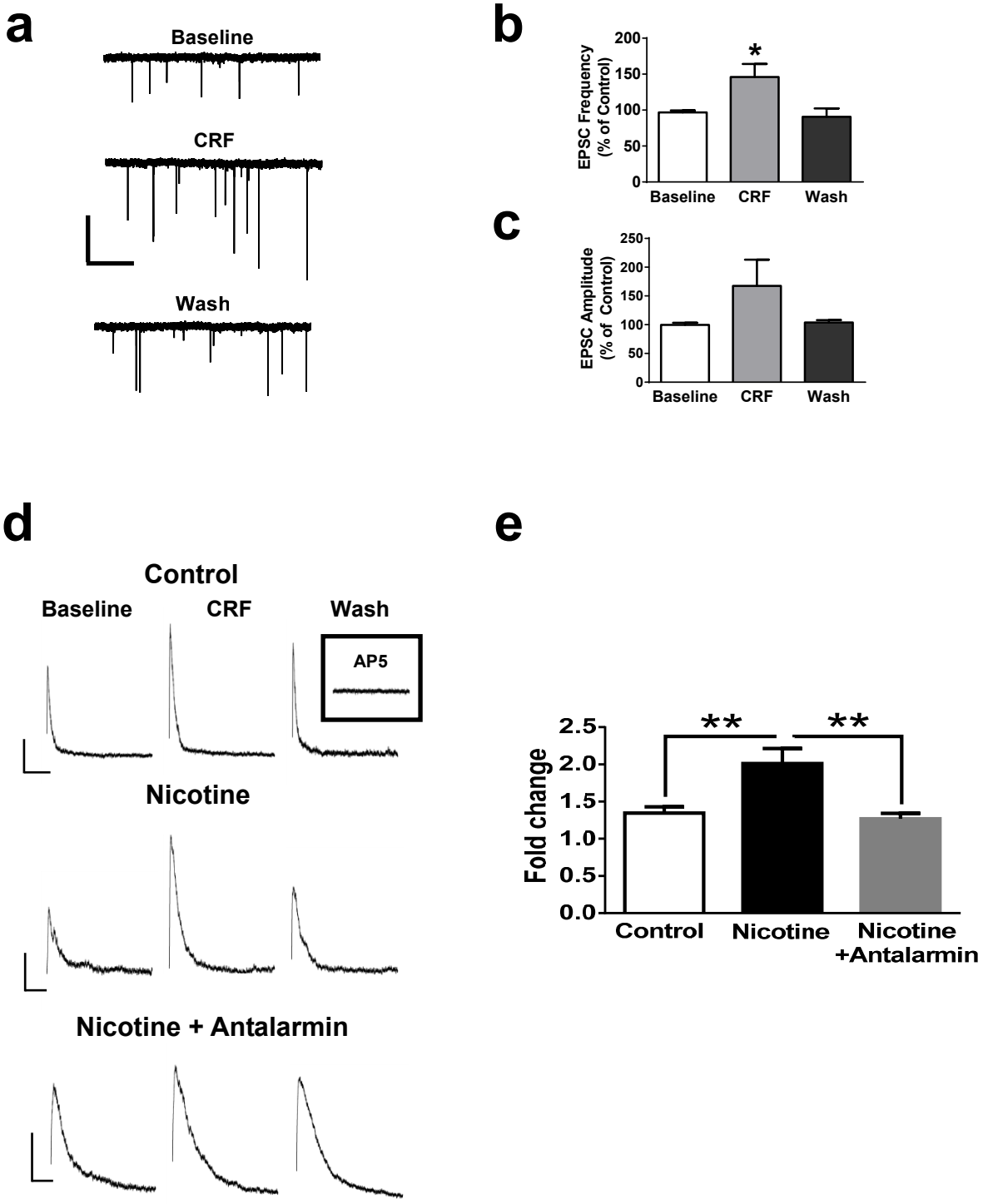
a
Baseline
CRF
Wash
b
EPSC Frequency (% of Control)
200
150
100
50
0
*
Baseline
CRF
Wash
c
EPSC Amplitude (% of Control)
250
200
150
100
50
0
Baseline
CRF
Wash
d
Control
Baseline
CRF
Wash
AP5
Nicotine
Nicotine + Antalarmin
e
Fold change
2.5
2.0
1.5
1.0
0.5
0.0
**
**
Control
Nicotine
Nicotine +Antalarmin

Supplementary Figure 6. CRF modulation of sEPSC and NMDA receptors. **a.** Representative whole-cell voltage clamp recordings from Type 2 neurons within the IPI of nicotine withdrawn slices in response to 250 nM CRF. Average sEPSC (**b.**) frequency and (**c.**) amplitude at baseline, after a 5-minute application of CRF, and after washout from Type 2 IPI neurons (n = 5, One-way ANOVA with repeated measures: Frequency, $p = 0.024$; Amplitude, NS). **d.** Representative electrically evoked NMDA currents from IPI neurons recorded in slices from nicotine naïve (top, Control) and chronic nicotine-treated (middle, Nicotine) mice. NMDA current (V_m = +40 mV) at baseline, after 5 min application of 250 nM CRF, and after 10 min washout are shown. Bottom, representative electrically evoked NMDA current from IPI neurons as described above except in the presence of antalarmin. Evoked currents were abolished in the presence of AP5 (10 μM, inset). Stimulation artifacts were removed for clarity. **e.** Average fold-change of peak evoked NMDA current in response to CRF (CRF response normalized to baseline) for control, chronic nicotine slices, and chronic nicotine slices in the presence of antalarmin. (n = 10, 8, and 8 neurons, respectively. Control vs. Nicotine: $t_{16} = 3.27$, $p = 0.0048$, two-tailed Student's t-test. Nicotine vs. Nicotine+Antalarmin: $t_{14} = 3.44$, $p = 0.004$). Data are expressed as mean ± SEM. *$p < 0.05$, **$p < 0.001$.

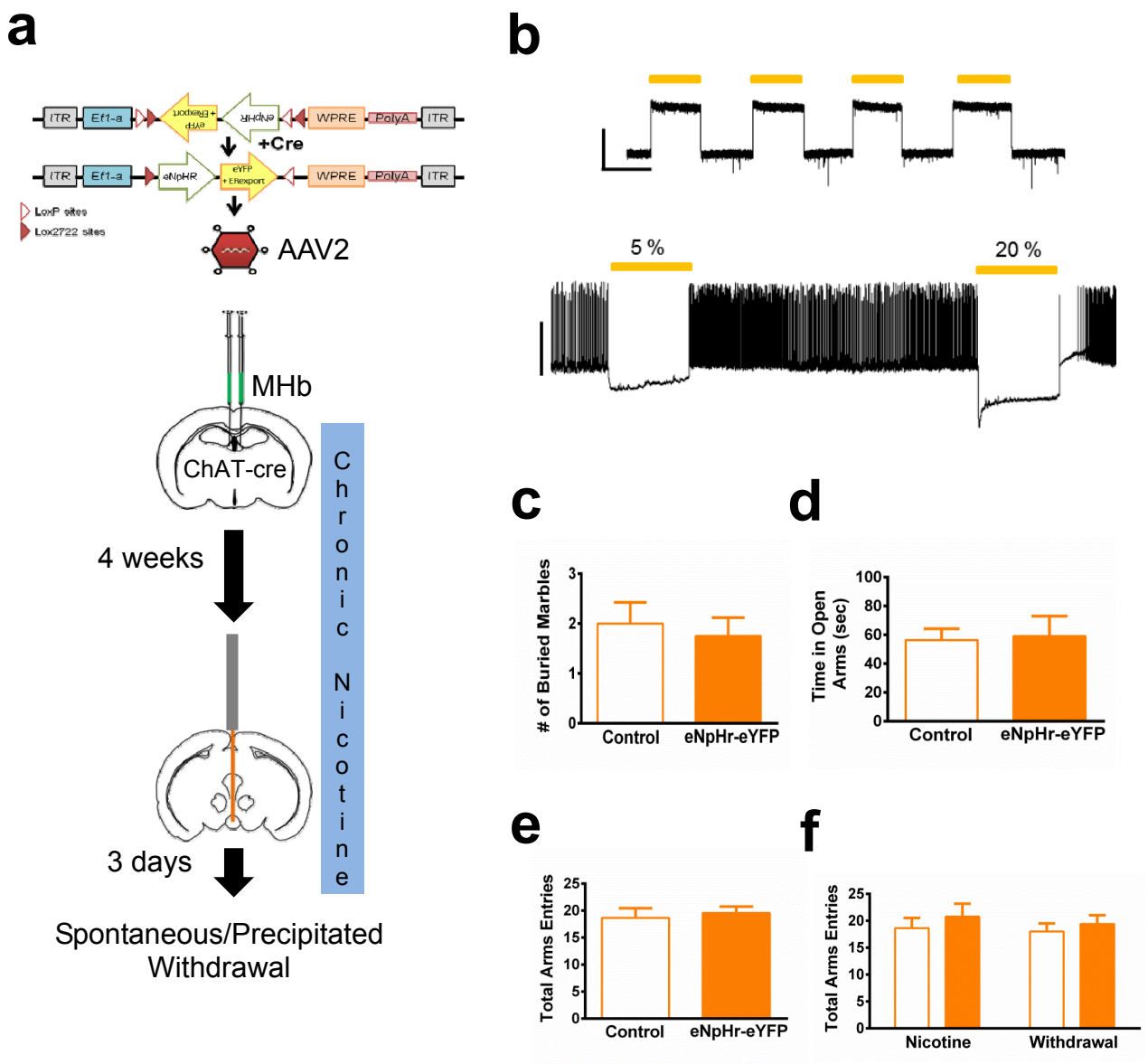

Supplementary Figure 7. Experimental paradigm for Halorhodopsin expression in MHb. **a.** Depiction of experimental strategy for expression of halorhodopsin selectively in cholinergic neurons of the MHb. The AAV-Ef1A-DIO-eNpHR-eYFP plasmid (top) allows for expression of halorhodopsin in neurons that express cre recombinase. The plasmid was packaged into AAV2 viral particles and injected bilaterally in the MHb of ChAT-cre

mice. Mice were then chronically treated with nicotine for 4 weeks. Optic cannulas targeting the MHb projections to the IPN were implanted and experiments examining activation of the IPI during mecamylamine-precipitated withdrawal or anxiety-like behavior during spontaneous nicotine withdrawal were conducted three days later. **b.** Representative whole-cell recordings from eYFP-positive MHb neurons under voltage-clamp (top) or current-clamp (bottom) in slices taken from eNpHR-eYFP infected ChAT-cre mice. Halorhodopsin was activated by 593 nm light indicated by the yellow bars. Top scale bar: x=100 pA, y=10s. Bottom scale bar: 50 mV. Baseline anxiety-like behavior in the **c.** MBT and **d.** EPM. in control-virus and eNpHR-eYFP-infected ChAT-cre mice during chronic nicotine treatment. **e.** Total arm entries from mice in panel d. **f.** Total arm entries in the EPM for mice in Figure 6f.

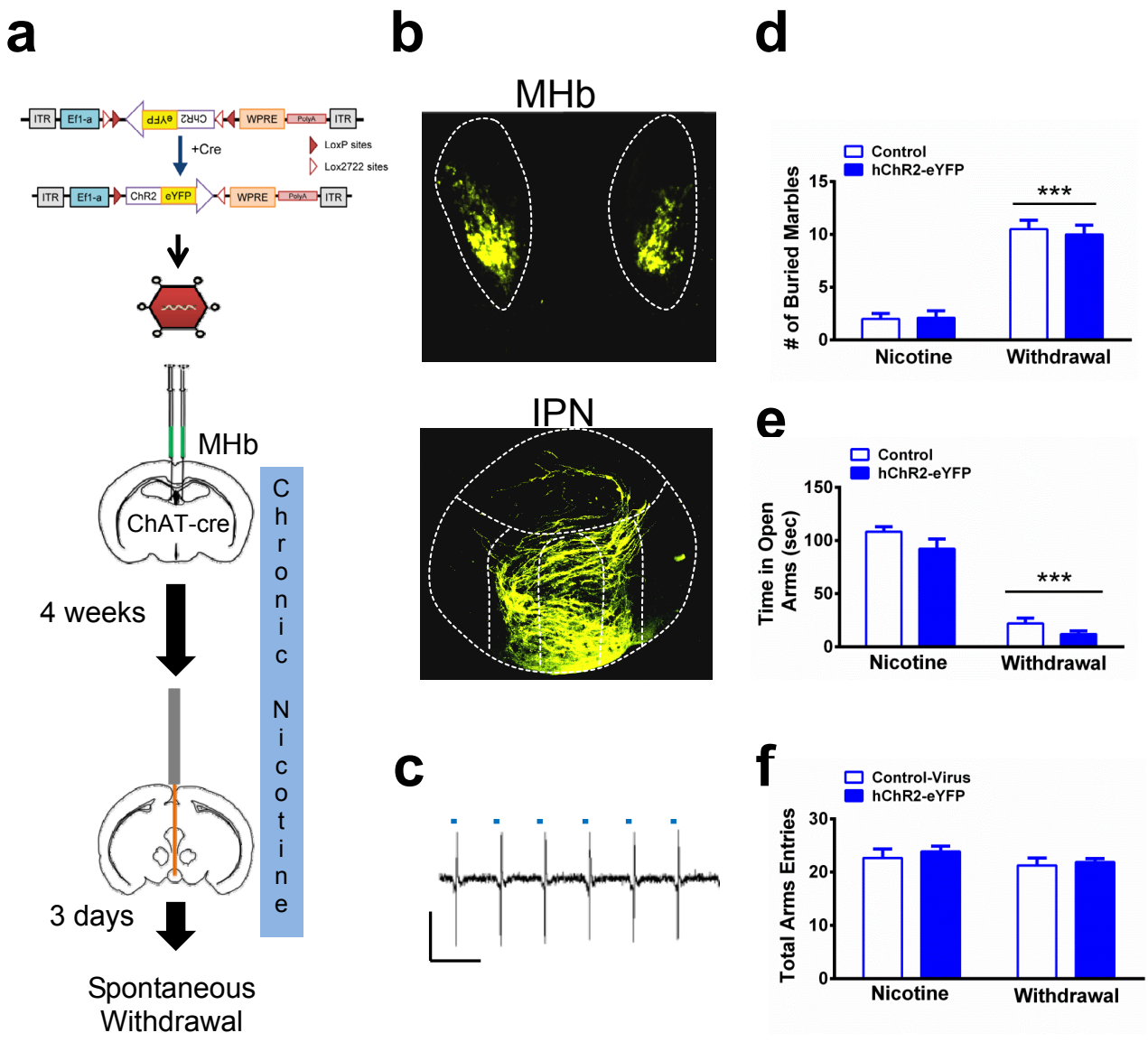

Supplementary Figure 8. Stimulation of MHb-IPN terminals does not reduce anxiety-like behavior in nicotine dependent mice. **a.** Experimental strategy for expression of channelrhodopsin in MHb ChAT neurons. AAV-Ef1A-DIO-ChR2-eYFP plasmid was packaged into AAV2 viral particles and injected into the MHb of ChAT-cre mice. **b.** Representative photomicrographs from representative MHb (top) and IPN (bottom)

coronal sections from ChAT-cre mice expressing ChR2-eYFP four weeks post-injection. **c.** Blue light-induced (blue bar = 2 ms light pulse) action potentials in MHb neurons expressing ChR2. Recordings were done in cell-attached patch-clamp mode. Scale bar: x = 50 ms, y = 20 pA. **d.** Number of marbles buried in nicotine-dependent, non-withdrawn (Nicotine) or nicotine-dependent, spontaneous withdrawn ChAT-cre mice (Withdrawal) expressing either control virus (Control, n = 9 and 12, respectively) or channelrhodopsin (ChR2-eYFP, n = 9). Behaviors in all groups were measured during light stimulation. Stimulation paradigm: 5 Hz, 50 ms pulse width, 35 m light-on epochs. **e.** Time spent on the open arms of the EPM in nicotine-dependent, non-withdrawn (Nicotine) or nicotine-dependent, spontaneous withdrawn ChAT-cre mice (Withdrawal) expressing either control virus (Control, n = 9 and 12, respectively) or ChR2-eYFP (n = 9 and 8, respectively). Behaviors in all groups were done during light stimulation. **f.** total arm entries in the EPM for each group. Data are expressed as mean ± SEM. Two-way ANOVA. ***$p < 0.001$, significant main effect of withdrawal state only (MBT: $F_{1, 34} = 112.9$. EPM: $F_{1, 34} = 187.7$).

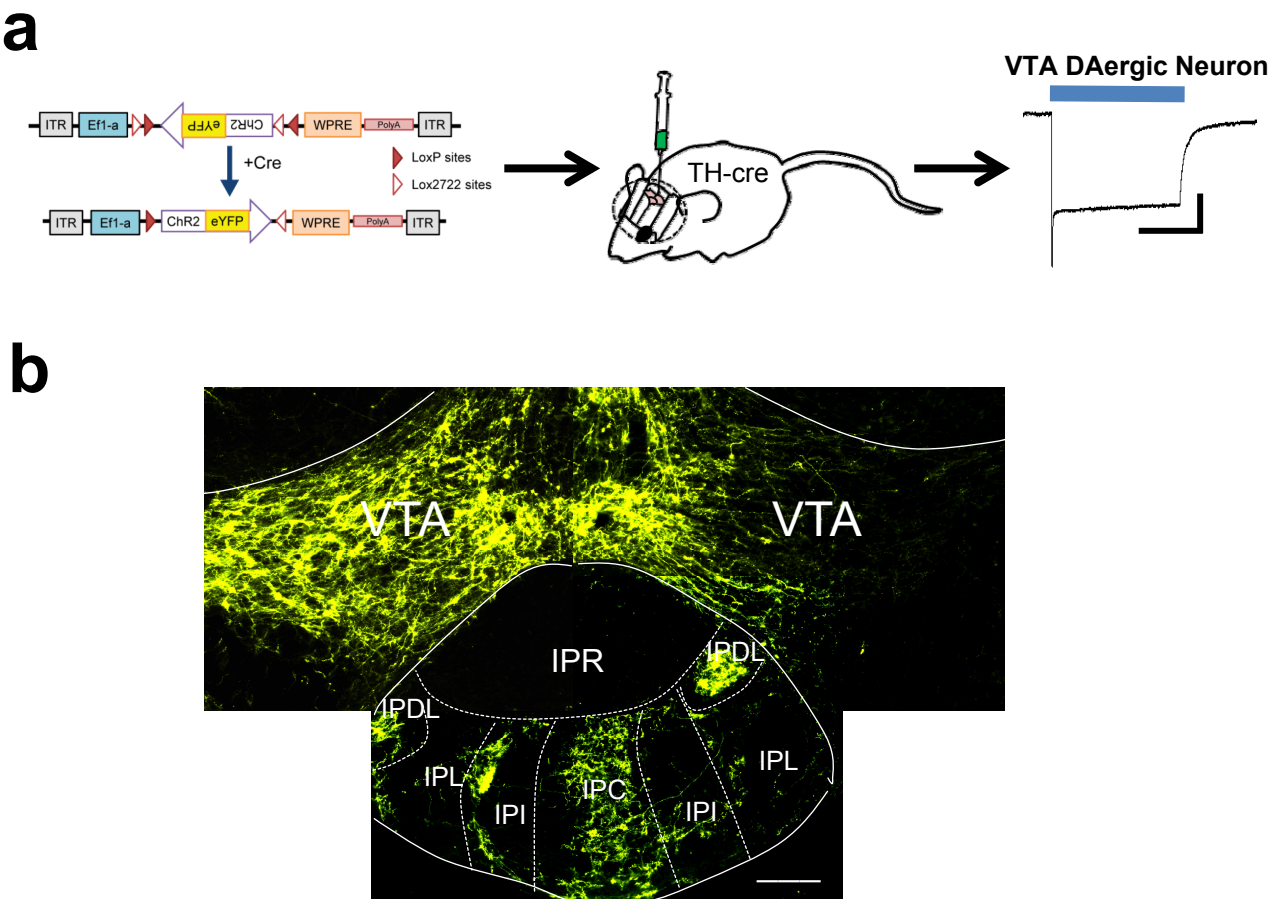

Supplementary Figure 9. A population of DAergic VTA neurons project to ventral IPN forming a meso-interpeduncular circuit. **a.** Experimental strategy for expression of channelrhodopsin in VTA DAergic neurons. AAV-Ef1A-DIO-ChR2-eYFP plasmid was packaged into AAV2 viral particles and injected into the VTA of TH-cre mice. Three to four weeks post-injection, VTA DAergic neurons robustly expressed ChR2 as indicated by blue light-induced inward currents under voltage-clamp at -70 mV (right). Scale bar: y = 200 pA, x = 1 s. **b.** Photomicrographs depicting eYFP signal in the VTA and IPN of TH-cre mice after unilateral injection of AAV2-ChR2-eYFP viral particles in the VTA. Scale bar: 200 μm.

Supplementary Table 1. Average sEPSC frequency and amplitude from data in Figure 4

	Neuron Type 1			Neuron Type 2		
	Mean sEPSC Frequency ± SEM (Hz)					
Treatment	Baseline	Response	Wash	Baseline	Response	Wash
CRF	4.43±0.91	4.40±0.91	4.25±0.86	2.38±0.87	3.47±1.25*	2.36±0.92
Antalarmin	2.58±0.60	2.29±0.58	2.53±0.58	2.14±0.65	1.46±0.43**	1.99±0.55
	Mean sEPSC Amplitude ± SEM (pA)					
CRF	10.76±1.72	11.47±1.78	11.27±1.82	10.91± 1.84	14.33± 1.97**	10.86±1.90
Antalarmin	12.03±1.32	12.13±1.84	12.23±1.82	12.58± 1.55	9.30± 1.01**	12.57±1.90

* $p < 0.05$, ** $p < 0.01$, drug treatment compared to baseline, One-way ANOVA with repeated measures, Bonferroni post-hoc